NANO LETTERS

Letter

pubs.acs.org/NanoLett

Single-Molecule Electric Revolving Door

Liang-Yan Hsu,*[,†] Elise Y. Li,*[,‡] and Herschel Rabitz*[,†]

[†]Department of Chemistry, Princeton University, Princeton, New Jersey 08544, United States

[‡]Department of Chemistry, National Taiwan Normal University, Taipei 11677, Taiwan

Supporting Information

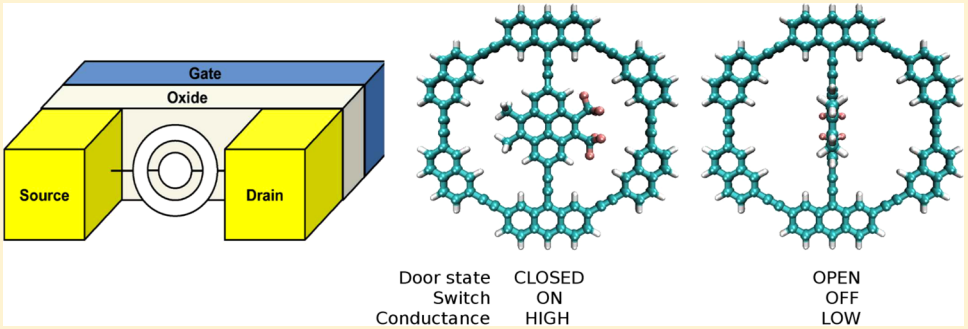

ABSTRACT: This work proposes a new type of molecular machine, the single-molecule electric revolving door, which utilizes conductance dependence upon molecular conformation as well as destructive quantum interference. We perform electron transport simulations in the zero-bias limit using the Landauer formalism together with density functional theory. The simulations show that the open- and closed-door states, accompanied by significant conductance variation, can be operated by an external electric field. The large on−off conductance ratio ($\sim 10^5$) implies that the molecular machine can also serve as an effective switching device. The simultaneous control and detection of the door states can function at the nanosecond scale, thereby offering a new capability for molecular-scale devices.

KEYWORDS: *Molecular machine, molecular electronics, quantum transport, conductance, molecular switch, density-functional theory*

Inspired by Richard Feynman's imaginative ideas half a century ago and motivated by examples discovered in nature, the field of molecular machinery has become an active area of research in nanoscience and synthetic chemistry. In the last two decades, a wide variety of artificial molecular machines have been reported including so-called molecular elevators,[1] shuttles,[2,3] rotors,[4−6] nanocars,[7,8] and turnstiles.[9−11] Among them, the molecular turnstiles have received considerable attention due to their resemblance to ordinary revolving doors. Most molecular turnstiles are based on phenyl-acetylene-macrocycles (PAMs)[9] or porphyrins.[10,11] The PAMs exhibit readable bistability revealed by NMR spectroscopy, but their open- or closed-door states could not be controlled by chemical reactions or temperature in solution. This problem was addressed in the porphyrin-based systems in which the opening and closing of the door can be operated by addition of competing ligands and metal ions. However, the complicated and slow switching mechanism appears to make it difficult to utilize such systems in durable devices. In this Letter, we show that, by combining concepts from molecular electronics[12−14] and molecular machinery, it is possible to control and detect the door states simultaneously, leading to a more versatile electromechanical component at the molecular level.

We propose a new type of molecular machine: a single-molecule electric revolving door (S-MERD), which utilizes conductance dependence upon molecular conformation as well as destructive quantum interference. The dependence of conductance upon molecular conformation is an important feature of electron transport through molecular junctions. Experimental studies have shown that the conductance of π-conjugated biphenyl systems varies as $\sim \sin^2\theta$ with the twist angle θ between the two phenyl rings.[15−17] This result, consistent with the ab initio calculations based on the nonequilibrium Green's function method and density functional theory,[16,18] implies that the magnitude of the tunneling current may be effectively controlled by changing the molecular conformation. In separate studies, destructive quantum interference with tunneling has been theoretically predicted in polyaromatic hydrocarbons (PAHs)[19−22] and experimentally observed in cross-conjugated molecular junctions.[23] On the basis of these prior works and inspired by the distinctive structure of the PAMs, we propose a series of PAM-based molecules (molecules **1**−**3**) and molecule **4** in Figure 1a as candidate systems for a S-MERD. The S-MERD concept exploits the synergistic effects of destructive quantum interference and molecular conformations upon single-molecule conductance.

Received: April 15, 2013
Revised: August 26, 2013

   dx.doi.org/10.1021/nl401340c | *Nano Lett.* XXXX, XXX, XXX−XXX

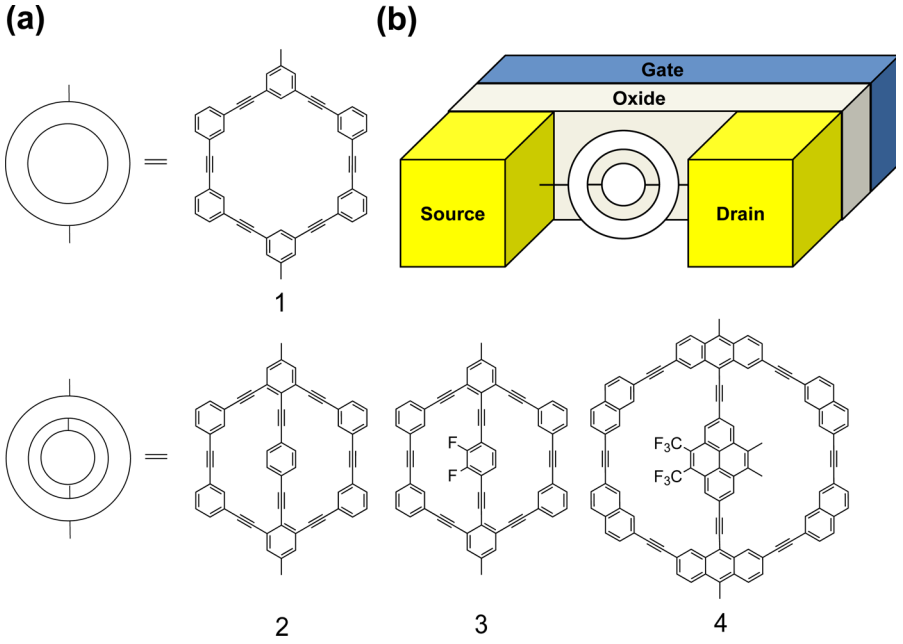

Figure 1. (a) Candidate molecules for the single-molecule electric revolving door (S-MERD). The schematic ring represents molecule **1**, while the schematic door including a door frame (the outer ring), a door (the inner plate) and two axles (the triple bonds) represents molecules **2**−**4**. (b) Illustration of a S-MERD. Molecules **1**−**4** are linked to two electrodes, the source and the drain, via a para-connection. The outer ring of molecules **2**−**4** is assumed to be parallel to the gate, and the inner plate can rotate around the axles.

Figure 1b illustrates that the S-MERD is a composite system including a gate electrode and two electrodes coupled to a particular candidate molecule, for example, molecules **1**−**4**. The flat (perpendicular) conformations of molecules **2**−**4**, formed by a coplanar (perpendicular) inner plate with respect to the outer ring, correspond to the closed (open) states of the S-MERD. Note that there is no open or closed state for molecule **1**. For conceptual simplicity, in our simulations we assume that the outer ring, connected to two electrodes, is stationary and lies parallel to the gate, while the inner plate can rotate around the triple-bond axles, that is, the outer ring serves as a stator while the inner plate is a rotor. The rotation of the inner plate can be manipulated by a gate electric field via the electric-dipole interaction. Thus, the switching speed of the door states, based on molecular rotational time scales (approximately $10^{-9} \sim 10^{-12}$ s), can reach the gigahertz scale.[24] In addition, it has also recently been shown that the measurement of electron transport through gold wires can reach the nanosecond time scale.[25] The two criteria combined together imply that the door states may be controlled and detected simultaneously. Provided that molecules **1**−**4** can be attached to the electrodes, then two particular issues arise: (I) The means to detect the open and closed states of the revolving door. (II) An assessment of the electron tunneling pathways, that is, does the tunneling electron pass through the revolving door along the outer ring, the inner plate, or both?

To address these two issues, we performed density functional theory calculations in the zero-bias limit to explore electron transport through molecules **1**−**4**. The quantum conductance is computed by the Landauer formula,[26,27] $G = [(2e^2)/h]T(E_F)$, where $T(E_F)$ is the transmission function for the system at the Fermi level. Note that the theoretical analysis applied here only holds in the coherent elastic tunneling regime, that is, no energy or phase loss happens in the transport process. The analysis is suitable for molecules with short chain length and large injection gaps, such as molecules **1**−**4**, because they have a short Landauer−Büttiker tunneling time.[28,29] In addition, prior experiments indicate that conductance changes resulting from inelastic tunneling via molecular vibrations are very small under off-resonant conditions,[30] and at low bias vibrationally induced decoherence cannot lead to any significant variations of tunneling current.[31] The transmission function is computed using the single-particle Green's function method, $T(E) = \mathrm{Tr}(\Gamma_L G^R_{mol} \Gamma_R G^A_{mol})$, where $G^{R(A)}_{mol}$ is the retarded (advanced) molecular Green's function and $\Gamma_{L(R)}$ is the molecule-electrode coupling function for the left (right) electrode, that is, the imaginary part of the self-energy contributed from the electrodes. The molecular Green's functions of the H-terminated molecules **1**−**4** are derived from the density-functional method in a maximally localized Wannier function (MLWF) representation[32,33] using the Quantum-ESPRESSO distribution[34] and the Wannier90[32] code.

For the electrodes, we adopt the wide-band-limit (WBL) approximation and neglect the real part of the self-energy, since we would like to explore the influence of molecular structure on transport properties and reduce other effects from the electrodes. The WBL approximation is appropriate as long as the electron density of states in the electrodes remains relatively flat around the Fermi level.[22] In addition, recent studies have confirmed that the WBL-metal, post-SCF, and full-SCF approaches all give similar and comparable results for aromatic molecules at zero bias.[35] These approximations allow the self-energy of the electrodes to be represented by a constant imaginary number and takes the form $\sum_{L(R)} = -i(\gamma_{L(R)}/2)|\alpha_{L(R)}\rangle\langle\alpha_{L(R)}|$, where $|\alpha_{L(R)}\rangle$ is the p_z orbital of the carbon atom linked to the left (right) electrode. The advantage of using the MLWF representation (rather than using a Gassian basis set that includes many polarization and diffuse functions for a single atom) is that it identifies the optimal $|\alpha_{L(R)}\rangle$ projector basis coupled to the electrodes so that one can single out the π- from σ-contribution to electron transport.[36] Here we set the coupling constant $\gamma_{L(R)}$ to be 0.5 eV, following typical

dx.doi.org/10.1021/nl401340c | Nano Lett. XXXX, XXX, XXX−XXX

estimates from other studies.[19,21] General computational details can be found in the Supporting Information regarding the functional and the basis set used in geometry optimizations and electron transport calculations.

The transmission spectra for molecule **1** and **2** in the WBL approximation are shown in Figure 2 in which the transmission

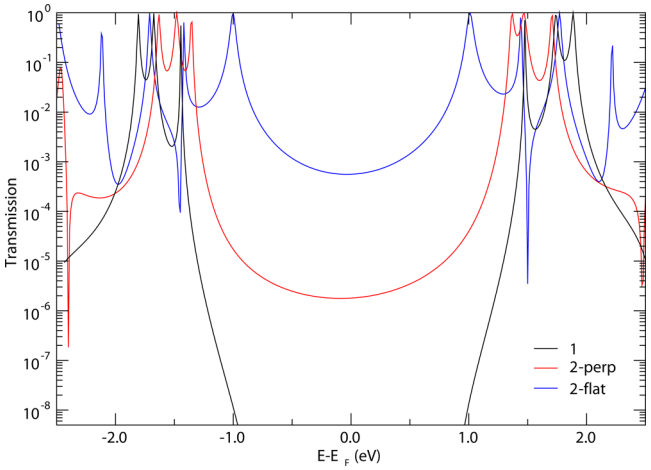

Figure 2. The transmission spectra of molecule **1** (the black line) and molecule **2** with central benzene in the perpendicular (the red line) or flat conformation (the blue line), where the abscissa is the energy of the tunneling electron with respect to the Fermi level.

peaks correspond to molecular orbitals of isolated H-terminated molecules (see the Supporting Information). For all molecules, we assume that the Fermi level lies at the midgap between the highest occupied molecular orbital (HOMO) and the lowest unoccupied molecular orbital (LUMO) when the molecules are connected to the two electrodes. It can be seen from Figure 2 that the transmission of **1** is highly suppressed (to below 10^{-8}) at energies between the HOMO and the LUMO that lie approximately 1 eV above and below the Fermi level, respectively. The wide range of transmission suppression of molecule **1**, showing that a tunneling electron from the source cannot pass through the outer ring to arrive at the drain, originates from destructive quantum interference caused by the meta-connected benzene units in molecule **1**.[19,20,22] In contrast, the inner plate of molecule **2**, the para-connected benzene, provides an additional transmission pathway for the tunneling electron when it is coplanar to the outer ring (**2**-flat), resulting in a significant increase in the transmission by a factor of approximately 10^5 compared to **1**. When the central benzene becomes perpendicular to the outer ring (**2**-perp), the π-orbitals of the central plate become orthogonal to those of the outer ring[18] and give rise to a transmission that is roughly 10^2 times lower than that of **2**-flat. The transmission of **2**-perp around the Fermi level, however, is still considerably larger than that of **1** due to additional electron transport facilitated by the overlap between the σ-orbitals of the inner plate and the π-orbitals of the outer ring.

The large on−off transmission ratio ($\sim 10^2$) of **2**-flat to **2**-perp at the Fermi level indicates that the open- and the closed-door states can be easily differentiated based on their quantum conductance and that molecule **2** may be used for a switching device. In addition, since this large on−off transmission ratio remains for a wide energy range (about 1 eV above and below the Fermi level), the slight Fermi level tuning introduced by the presence of the electrodes should not affect this phenomenon, that is, the choice of electrodes is not a crucial issue for the S-MERD. However, the inner plate of molecule **2** lacking a permanent dipole moment means that it cannot be operated by the gate. A permanent dipole may be introduced by substituting electron-withdrawing or electron-donating groups, for example, fluorine atoms (molecule **3**) or methyl groups, for the hydrogen atoms of the inner plate. Ideally, molecules **2** and **3** should have the lowest energy when the inner rotor and outer stator are coplanar so that the entire set of π-electrons is conjugated. The potential energy is expected to increase as the inner benzene gradually rotates out of planarity since the π-conjugation decreases and to reach the highest energy barrier in the perpendicular conformation. But for both **2** and **3**, the strong steric repulsion between the hydrogen atoms of the outer ring and the hydrogen (fluorine) atoms of the inner benzene (the distance $\lesssim$1.8 Å) significantly raises the energy of the flat configuration. Geometry optimization predicts that the most stable structure for both **2** and **3** is a tilted conformation with a twist angle of about 40° between the inner benzene and the outer ring. In addition, the strong repulsion between the inner plate and the outer ring also causes a significant distortion for molecule **3**, forcing the outer ring to adopt a nonplanar geometry.

To solve this problem, we consider molecule **4** that has not been synthesized to our knowledge. For molecule **4** with a permanent dipole (including two trifluoromethyl and two methyl groups), the outer ring exhibits similar destructive quantum interference properties and offers larger room for the inner pyrene rotor. Note that molecule **4** shares a characteristic feature with molecules **2** and **3**: the length of the inner plate added to the two acetylenic axles is equal to the inner diameter of the outer ring,[9] suggesting that molecule **4** can be possibly synthesized. We hope that these results motivate the synthesis of single-molecule electric revolving doors with suitable novel structure along the lines of molecule **4**. In addition, molecule **4** gives the highest and the lowest transmission in the flat and the perpendicular conformations, respectively. The transmissions for the two conformations are characterized by an extremely high on−off π-transmission ratio for $\gtrsim 10^5$ as shown by the solid curves in Figure 3. This large on−off π-transmission ratio also remains for a wide energy range between the HOMO and the LUMO and therefore is not sensitive to the Fermi level of the electrodes.

Note that in the current WBL approximation we only consider the coupling between the p_z orbital of the contact carbon atoms and the left (right) electrode, that is, the transmission originates purely from π-electrons. One may question whether only π-transmission is sufficient to capture the nature of electron transport through molecule **4**. To clarify this issue, we also computed pure σ-transmission for molecule **4** in the two conformations under the same molecule-electrode coupling strength 0.5 eV, as shown by the dashed curves in Figure 3. Figure 3 shows that the σ-transmissions are $\sim 10^3$−10^4 times smaller than their respective π-transmissions. This finding is consistent with the previous study, indicating that the contributions of σ-transmission are typically extremely small for a large conjugated system.[22] Even in the worst case scenario when the flat and perpendicular conformations are dominated by σ- and π-transmissions respectively, the on−off ratio of **4**-flat-σ to **4**-perp-π is still larger than 10^2.

Potential energy surface investigation of the isolated molecule **4** confirms that the flat configuration is the most

dx.doi.org/10.1021/nl401340c | *Nano Lett.* XXXX, XXX, XXX−XXX

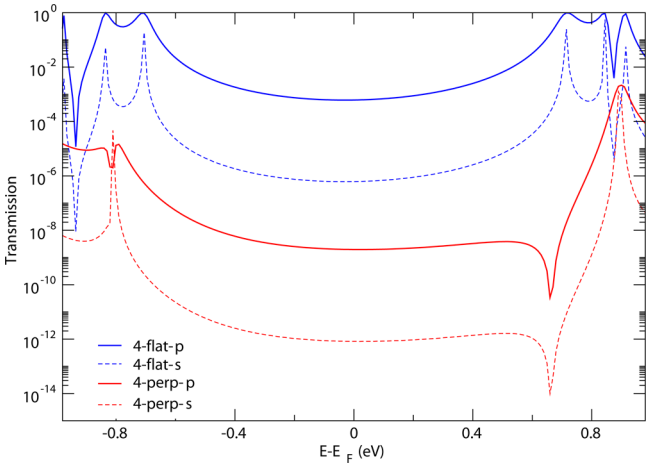

Figure 3. The transmission spectra of molecule **4** with a central pyrene rotor in the perpendicular (red curves) or flat conformation (blue curves), where the abscissa is the energy of the tunneling electron with respect to the Fermi level. Both the π- (solid curves) and σ- (dashed curves) transmissions are considered.

stable structure in the absence of the gate electric field and that the energy barrier between the flat and perpendicular conformations is ~170 meV, as shown in Figure 4a. With a

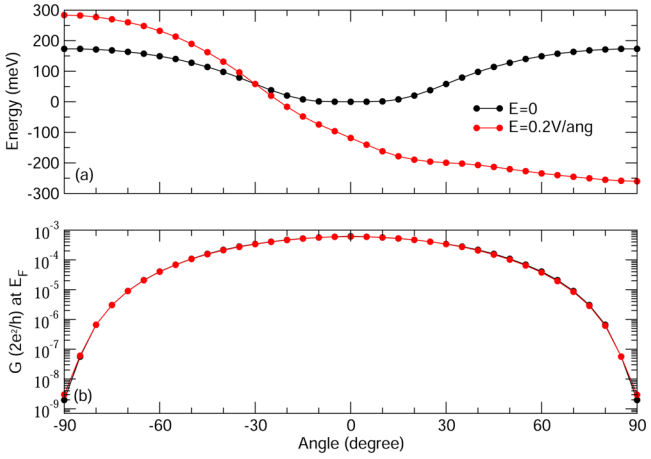

Figure 4. (a) The potential energy surface profile and (b) the quantum conductance at the Fermi level (lower panel) of molecule **4** with respect to the twist angle between the inner rotor and outer stator when no external electric field is applied (black curve) and when an external electric field (0.2 V/Å) is applied perpendicular to the outer ring surface. The values of the potential energy surface and the quantum conductance can be found in the Supporting Information.

sufficient gate electric field (~0.2 V/Å), the relative stability between the two conformations can be reversed. The red curve in Figure 4a shows that the potential energy of molecule **4** reaches the highest and the lowest at the 90° and −90°, when the permanent dipole of the inner pyrene rotor lies parallel and antiparallel to the gate electric field, respectively. Note that the open-door state with an E-dependent shallow potential energy around 90° may be affected by thermal fluctuations, although the energy difference between 0° and 90° with the gate electric field is over 140 meV, five times larger than $kT \sim 26$ meV at room temperature. The relatively large gate electric field of 0.2 V/Å shows that the open-door state can be fully reached, in principle. However, the typical breakdown electric field of oxide layers, such as Al_2O_3, is about 0.1 V/Å, above which leakage current occurs. This issue may be avoided by the choice of a molecular rotor with a larger dipole moment or a smaller energy difference between the flat and perpendicular conformations.

Figure 4b shows that the quantum conductance increases gradually from the perpendicular (90° or −90°) to the flat conformation and there is nearly zero effect on the conductance from the gate electric field. The large on−off conductance ratio of the flat to perpendicular conformation is consistent with the transmissions at the Fermi level in Figure 3. Therefore, molecule **4** fulfills the requirements for a good S-MERD and an effective switching device. In the absence of the gate electric field, molecule **4** exists in the stable flat conformation (the closed-door state) and exhibits maximal conductance, corresponding to the on-state for a switch. In the presence of the gate electric field ($\gtrsim$ 0.2 V/Å), the inner plate rotates to the perpendicular conformation (the open-door state) and exhibits minimal conductance, corresponding to the off-state for a switch. Note that although the door state of molecule **4** cannot fully reach 90° under a weaker electric field $\lesssim$0.15 V/Å, the conductance variation with respect to molecular conformation can be still used as the basis for a switching device, for example, the on−off conductance ratio of the 0° to the 60° conformation is roughly 10.

In an experiment, the single-molecule conductance may be influenced by the contact geometries and electrode inhomogeneities. To account for the average effects of these factors, we modeled the self-energy of the electrodes as a function of random variables, that is, $\sum(E_F) = |\alpha_L\rangle\Delta_L - i(\gamma_L/2)\langle\alpha_L| + |\alpha_R\rangle\Delta_R - i(\gamma_R/2)\langle\alpha_R|$, where Δ_L and Δ_R are each chosen randomly from −4 to 4 eV, and γ_L and γ_R are each chosen randomly from 0.1 to 4 eV. Note that in the current study we consider a zero-bias conductance so $\sum(E) = \sum(E_F)$ = constant, and typically $\Delta_{L(R)}$ and $\gamma_{L(R)}$ are chosen as 0 and 0.5 eV, respectively, in the WBL approximation. As a result, this method enables the modeling of large variations of the electrode inhomogeneities and the molecule-lead contacts without performing full electrode-molecule-electrode calculations. Furthermore, the modeling is more representative than a large-scale full atomistic simulation based on only one or two specific lead and molecular geometries. Figure 5 shows the histogram of 4000 conductance calculations for molecule **4** with random values for the self-energies of the left and right electrodes in the absence or presence of an electric field. Even for such a significant variation of the electrode self-energies, the conductance histograms of the closed-door and open-door states are still completely separated from each other. These computations indicate that differentiation between the closed- and open-door states is robust with these practical experimental considerations. In addition, we also explored the influence of geometry fluctuations of molecule **4** at temperatures of 4 and 77 K on the single-molecule conductance using the atom-centered density matrix propagation (ADMP) method[37] at the semiempirical PM3MM level in the Gaussian 09 program.[38] Our computations show that at 4 and 77 K the conductance histograms of the closed- and open-door states are well-separated, indicating that the two states can be readily differentiated. The computational details and results can be found in the Supporting Information.

In the current study, we have shown that π-transmission dominates the electron transport mechanism through molecule **4** and that the large on−off transmission ratio is not sensitive to

dx.doi.org/10.1021/nl401340c | Nano Lett. XXXX, XXX, XXX−XXX

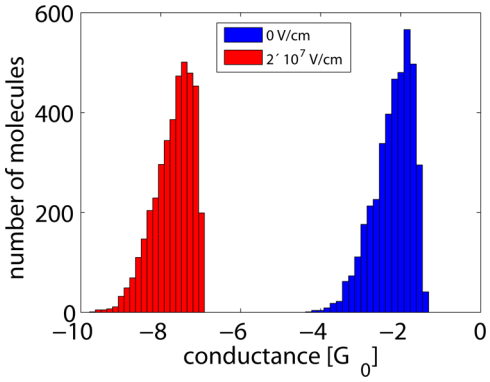

Figure 5. Conductance histograms derived from 4000 conductance calculations for molecule **4** with random values for the self-energies of the left and right electrodes, where the abscissa is the conductance on a logarithmic scale and $G_0 = 2e^2/h$. The blue and red histograms correspond to the conductance of the closed-door and open-door states with corresponding average conductances of $1.04 \pm 0.88 \times 10^{-2}G_0$ and $3.34 \pm 2.78 \times 10^{-8}G_0$.

the Fermi level of the electrodes. We adopt the WBL approximation, assuming a constant density of states around the Fermi level of the electrode and estimate the relative contribution between σ- and π-transmission using the same coupling strength. However, the molecule-electrode coupling strength is a function of the electron density of states in the electrodes, and the relative coupling strength between the σ- and π-orbitals can depend on the chemical nature of the electrode and the linker groups. For example, a thiol linkage to a gold electrode may preferentially facilitate the σ-transmission while a metallic carbon nanotube electrode directly coupled to conjugate molecules primarily facilitates the π-transmission. To explore the most suitable electrode for the experimental setup, a full electrode-molecule-electrode calculation including the atomistic details of molecule-electrode contact would be required.

In summary, drawing on inspirations from molecular electronics, we present a general principle for designing a special type of S-MERD. The influence of molecular conformation and destructive quantum interference on single-molecule conductance has been illustrated in molecules **1**−**4**. The computational results show that the door states of molecule **4** can be readily differentiated without ambiguity by their conductance difference, and its large on−off conductance ratio ($\sim 10^5$) can be used for an effective switching device. In addition, simultaneous control and detection of the door states indicate that it should be possible to manipulate such molecular machines on the nanosecond scale. We believe that this study provides new directions for experimental and theoretical investigations into S-MERDs and other related molecular machines. Future studies could include searching for better candidate S-MERDs, whose door states can be operated under weaker electric fields (<0.1 V/Å). We hope that this work motivates further consideration of combining molecular machinery and molecular electronics to explore novel nanotechnology devices and applications.

■ ASSOCIATED CONTENT

Ⓢ Supporting Information

The computational details, the electronic structure of model systems, the conductance histograms of molecule **4** at 4 and 77 K, and the potential energy surface of molecule 4. This material is available free of charge via the Internet at http://pubs.acs.org.

■ AUTHOR INFORMATION

Corresponding Authors

*E-mail: (L.-Y.H.) lianghsu@princeton.edu.
*E-mail: (E.Y.L.) eliseytli@ntnu.edu.tw.
*E-mail: (H.R.) hrabitz@princeton.edu.

Notes

The authors declare no competing financial interest.

■ ACKNOWLEDGMENTS

L.-Y.H. thanks Professor Zoltan Soos and Professor Annabella Selloni for useful discussions. This research is supported by the NSF and ARO of the United States and the National Science Council of Taiwan, R.O.C.

■ REFERENCES

(1) Badjić, J. D.; Balzani, V.; Credi, A.; Silvi, S.; Stoddart, J. F. *Science* **2004**, *303*, 1845−1849.
(2) Bissell, R. A.; Córdova, E.; Kaifer, A. E.; Stoddart, J. F. *Nature* **1994**, *369*, 133−137.
(3) Panman, M. R.; Bodis, P.; Shaw, D. J.; Bakker, B. H.; Newton, A. C.; Kay, E. R.; Brouwer, A. M.; Buma, W. J.; Leigh, D. A.; Woutersen, S. *Science* **2010**, *328*, 1255−1258.
(4) Koumura, N.; Zijlstra, R. W. J.; Delden, R. A. v.; Harada, N.; Feringa, B. L. *Nature* **1999**, *401*, 152−155.
(5) Delden, R. A. v.; Wiel, M. K. J. t.; Pollard, M. M.; Vicario, J.; Koumura, N.; Feringa, B. L. *Nature* **2005**, *437*, 1337−1340.
(6) Ruangsupapichat, N.; Pollard, M. M.; Harutyunyan, S. R.; Feringa, B. L. *Nature Chem.* **2011**, *3*, 53−60.
(7) Shirai, Y.; Osgood, A. J.; Zhao, Y.; Kelly, K. F.; Tour, J. M. *Nano Lett.* **2005**, *5*, 2330−2334.
(8) Kudernac, T.; Ruangsupapichat, N.; Parschau, M.; Maciá, B.; Katsonis, N.; Harutyunyan, S. R.; Ernst, K.-H.; Feringa, B. L. *Nature* **2011**, *479*, 208−211.
(9) Bedard, T. C.; Moore, J. S. *J. Am. Chem. Soc.* **1995**, *117*, 10662−10671.
(10) Lang, T.; Guenet, A.; Graf, E.; Kyritsakas, N.; Hosseini, M. W. *Chem. Commun.* **2010**, *46*, 3508−3510.
(11) Lang, T.; Graf, E.; Kyritsakas, N.; Hosseini, M. W. *Dalton Trans.* **2011**, *40*, 3517−3523.
(12) Liang, W.; Shores, M. P.; Bockrath, M.; Long, J. R.; Park, H. *Nature* **2002**, *417*, 725−729.
(13) Nitzan, A.; Ratner, M. A. *Science* **2003**, *300*, 1384−1389.
(14) Lindsay, S. M.; Ratner, M. A. *Adv. Mater.* **2007**, *19*, 23−31.
(15) Venkataraman, L.; Klare, J. E.; Nuckolls, C.; Hybertsen, M. S.; Steigerwald, M. L. *Nature* **2006**, *442*, 904−907.
(16) Mishchenko, A.; Vonlanthen, D.; Meded, V.; Bürkle, M.; Li, C.; Pobelov, I. V.; Bagrets, A.; Viljas, J. K.; Pauly, F.; Evers, F.; Mayor, M.; Wandlowski, T. *Nano Lett.* **2010**, *10*, 156−163.
(17) Mishchenko, A.; Zotti, L. A.; Vonlanthen, D.; Bürkle, M.; Pauly, F.; Cuevas, J. C.; Mayor, M.; Wandlowski, T. *J. Am. Chem. Soc.* **2011**, *133*, 184−187.
(18) Bürkle, M.; Viljas, J. K.; Vonlanthen, D.; Mishchenko, A.; Schön, G.; Mayor, M.; Wandlowski, T.; Pauly, F. *Phys. Rev. B* **2012**, *85*, 075417.
(19) Hsu, L.-Y.; Rabitz, H. *Phys. Rev. Lett.* **2012**, *109*, 186801.
(20) Hsu, L.-Y.; Jin, B.-Y. *Chem. Phys.* **2009**, *355*, 177−182.
(21) Cardamone, D. M.; Stafford, C. A.; Mazumdar, S. *Nano Lett.* **2006**, *6*, 2422−2426.
(22) Ke, S.-H.; Yang, W.; Baranger, H. U. *Nano Lett.* **2008**, *8*, 3257−3261.
(23) Guédon, C. M.; Valkenier, H.; Markussen, T.; Thygesen, K. S.; Hummelen, J. C.; Molen, S. J. v. d. *Nat. Nanotechnol.* **2012**, *7*, 305−309.
(24) Fleming, G. R.; Wolynes, P. G. *Phys. Today* **1990**, *43*, 36−43.

(25) Guo, S.; Hihath, J.; Tao, N. *Nano Lett.* **2011**, *11*, 927−933.
(26) Landauer, R. *Philos. Mag.* **1970**, *21*, 863−867.
(27) Meir, Y.; Wingreen, N. S. *Phys. Rev. Lett.* **1992**, *68*, 2512−2515.
(28) Nitzan, A.; Jortner, J.; Wilkie, J.; Burin, A. L.; Ratner, M. A. *J. Phys. Chem. B* **2000**, *104*, 5661−5665.
(29) Nitzan, A. *Annu. Rev. Phys. Chem.* **2001**, *52*, 681−750.
(30) Song, H.; Kim, Y.; Jeong, H.; Reed, M. A.; Lee, T. *J. Phys. Chem. C* **2010**, *114*, 20431−20435.
(31) Ballmann, S.; Härtle, R.; Coto, P. B.; Elbing, M.; Mayor, M.; Bryce, M. R.; Thoss, M.; Weber, H. B. *Phys. Rev. Lett.* **2012**, *109*, 056801.
(32) Mostofi, A. A.; Yates, J. R.; Lee, Y.-S.; Souza, I.; Vanderbilt, D.; Marzari, N. *Comput. Phys. Commun.* **2008**, *178*, 685.
(33) Lee, Y.-S.; Marzari, N. *Phys. Rev. Lett.* **2005**, *95*, 076804.
(34) Giannozzi, P.; Baroni, S.; Bonini, N.; Calandra, M.; Car, R.; Cavazzoni, C.; Ceresoli, D.; Chiarotti, G. L.; Cococcioni, M.; Dabo, I.; et al. *J. Phys.: Condens. Matter* **2009**, *21*, 395502.
(35) Verzijl, C. J. O.; Seldenthuis, J. S.; Thijssen, J. M. *J. Chem. Phys.* **2013**, *138*, 094102.
(36) Li, E. Y.; Marzari, N. *J. Phys. Chem. Lett.* **2013**, *4*, 3039−3044.
(37) Schlegel, H. B.; Millam, J. M.; Iyengar, S. S.; Voth, G. A.; Daniels, A. D.; Scuseria, G. E.; Frisch, M. J. *J. Chem. Phys.* **2001**, *114*, 9758−9763.
(38) Frisch, M. J. et al. *Gaussian 09*, Revision A.1.; Gaussian Inc.: Wallingford CT, 2009.

dx.doi.org/10.1021/nl401340c | *Nano Lett.* XXXX, XXX, XXX−XXX